Electronic Supplementary Material (ESI) for Materials Horizons.

Electronic Supporting Information

Origin of Multiple Voltage Plateaus in P2-type Sodium Layered Oxides

Yang Gan,[ab] Yining Li,[ab] Haoxin Li,[abc] Wujie Qiu [ab] and Jianjun Liu*[abc]

[a]State Key Laboratory of High Performance Ceramics and Superfine Microstructure, Shanghai Institute of Ceramics, Chinese Academy of Sciences, 1295 Dingxi Road, Shanghai 200050, China

[b]Center of Materials Science and Optoelectronics Engineering, University of Chinese Academy of Sciences, Beijing 100049, China

[c]School of Chemistry and Materials Science, Hangzhou Institute for Advanced Study, University of Chinese Academy of Science, 1 Sub-lane Xiangshan, Hangzhou 310024, China

Corresponding Author

*Email: jliu@mail.sic.ac.cn

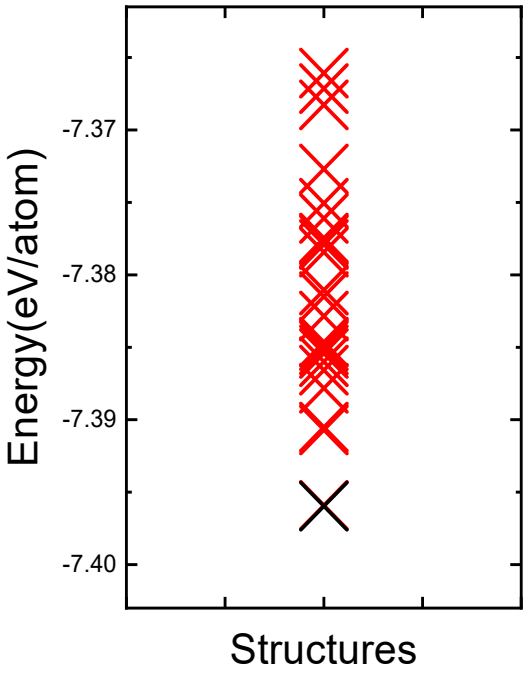

Figure S1. Disordered structures of P2-$Na_{0.6}[Cr_{0.6}Ti_{0.4}]O_2$. Relative energy distribution of all SQS disordered structures of $Na_{0.6}[Cr_{0.6}Ti_{0.4}]O_2$ after DFT relaxation. Black cross is the lowest energy structure.

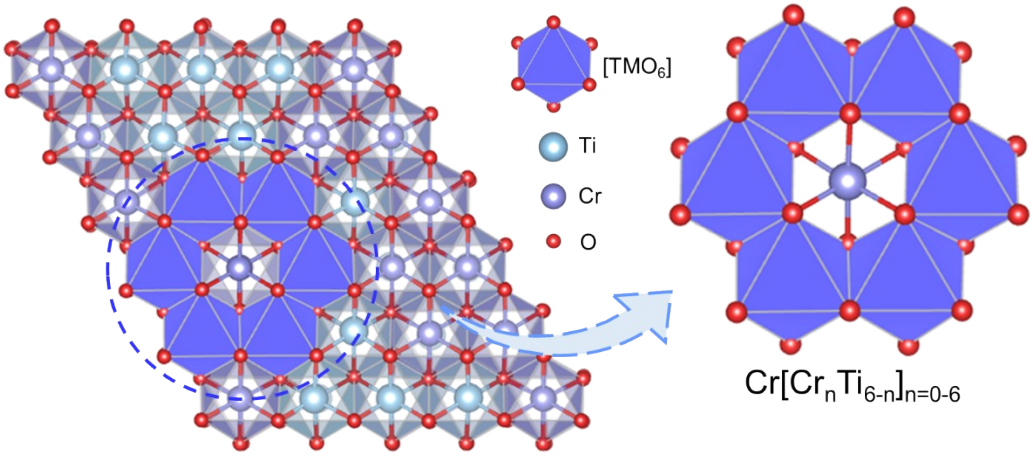

Figure S2. The honeycomb-like local structure $Cr[Cr_nTi_{6-n}]$ in the $Na_{0.6}[Cr_{0.6}Ti_{0.4}]O_2$

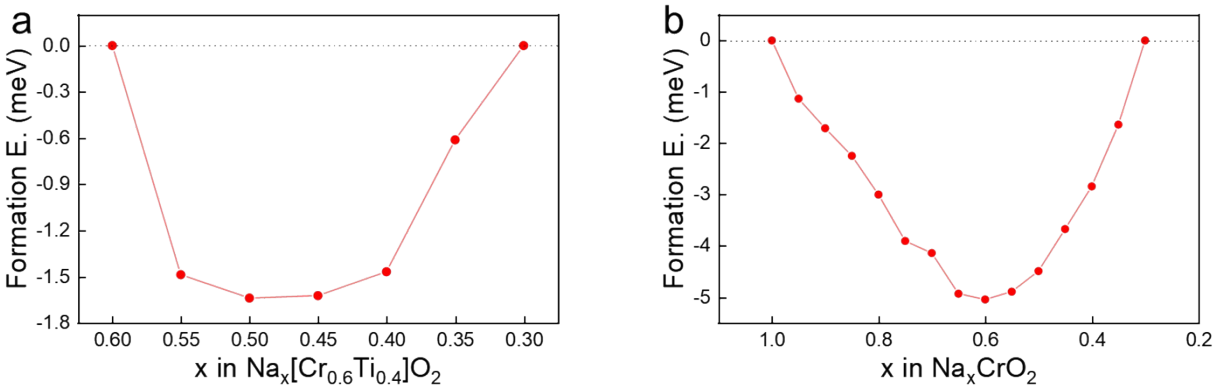

Figure S3. Formation energies indicate stable intermediate phases during the cycles of $Na_x[Cr_{0.6}Ti_{0.4}]O_2$ (x = 0.3-0.6) and Na_xCrO_2 (x = 0.3-1.0).

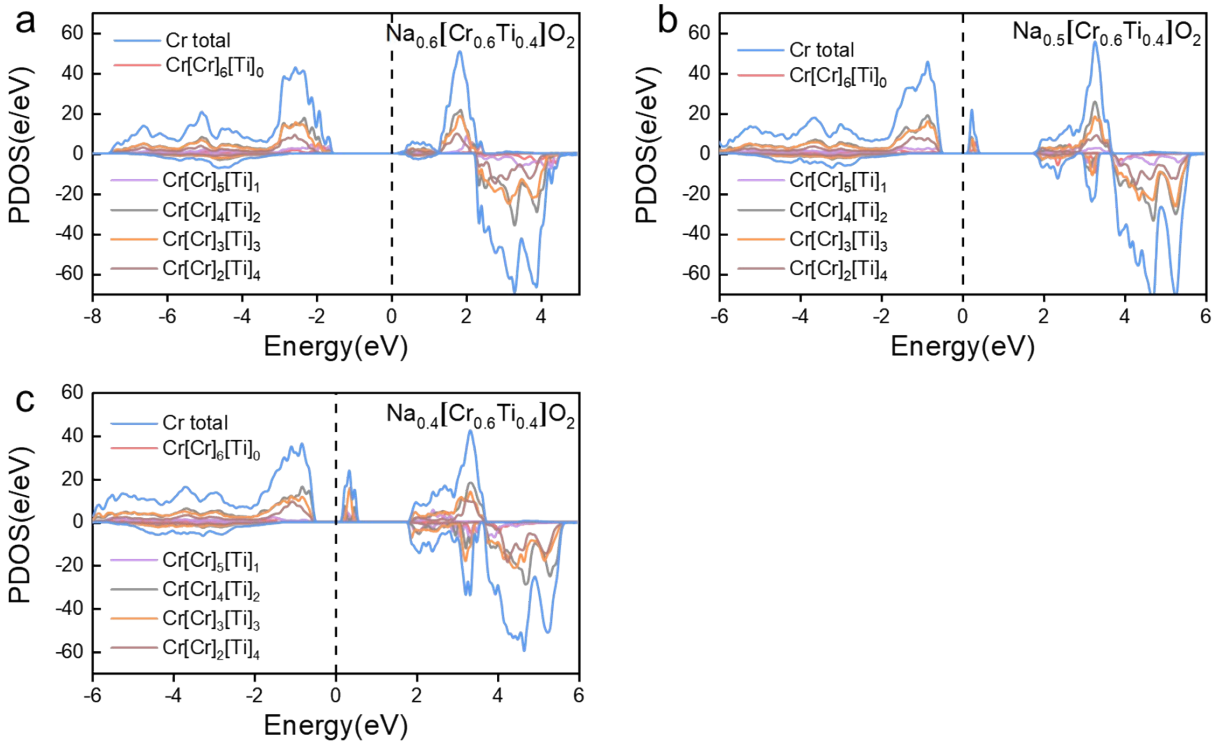

Figure S4. The partial density of states of different Cr in $Na_x[Cr_{0.6}Ti_{0.4}]O_2$(x=0.6,0.5,0.4), respectively.

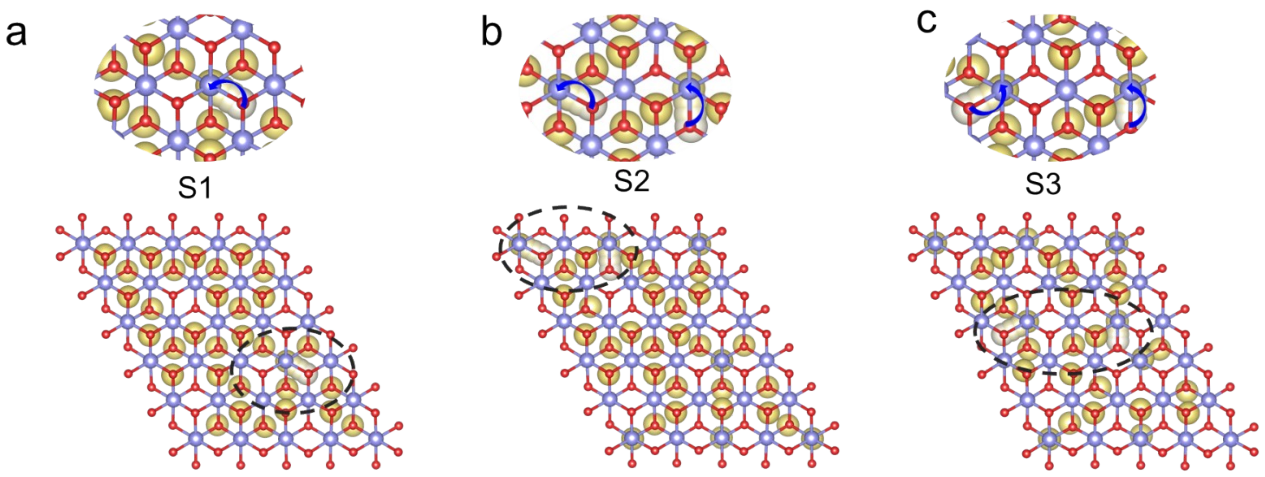

Figure S5. Na-ion migration from Na_e sites to Na_f sites at the voltage plateau S1, S2, S3, respectively. The blue arrows indicate the migration of sodium ions.

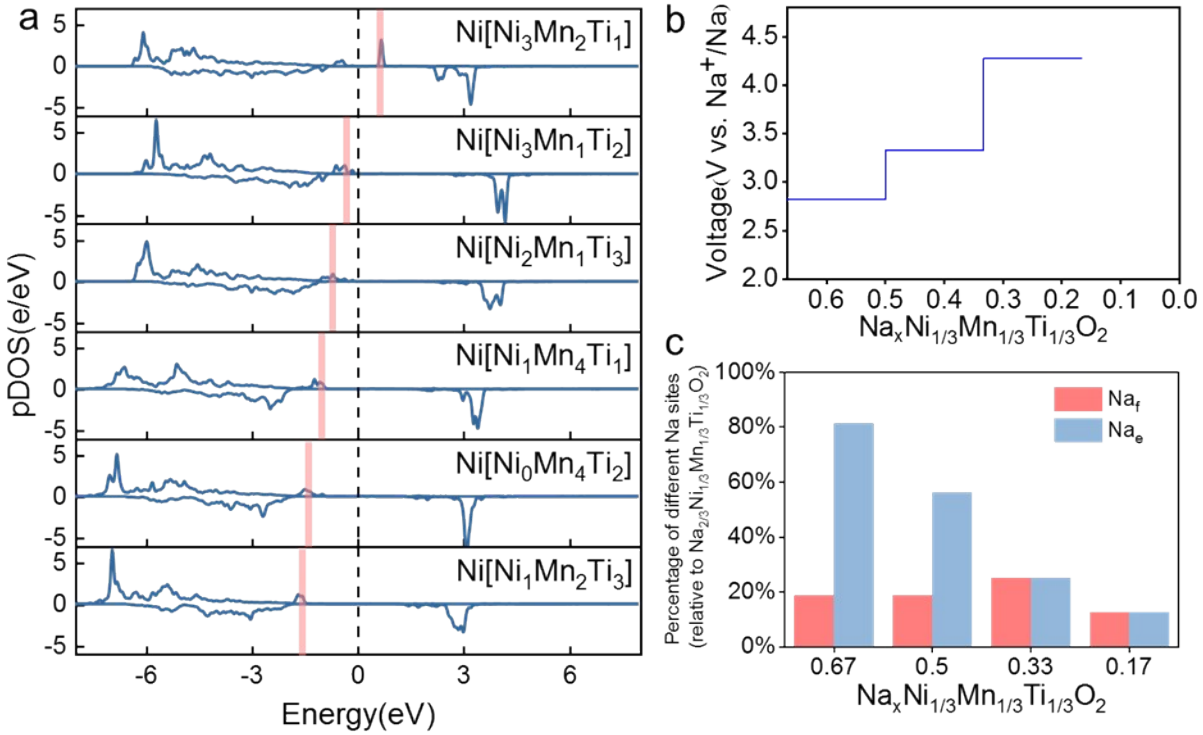

Figure S6. (a) Electronic structures of Ni in six typical honeycomb local structures $Ni[Ni_3Mn_2Ti_1]$, $Ni[Ni_3Mn_1Ti_2]$, $Ni[Ni_2Mn_1Ti_3]$, $Ni[Ni_1Mn_4Ti_1]$, $Ni[Ni_0Mn_4Ti_2]$ and $Ni[Ni_1Mn_2Ti_3]$ on $Na_{2/3}Ni_{1/3}Mn_{1/3}Ti_{1/3}O_2$; (b) Calculated charging voltages of $Na_{2/3}Ni_{1/3}Mn_{1/3}Ti_{1/3}O_2$; (c) Changes of the two Na sites within the structure of $Na_{2/3}Ni_{1/3}Mn_{1/3}Ti_{1/3}O_2$ (x=0.67, 0.5, 0.33, 0.17);

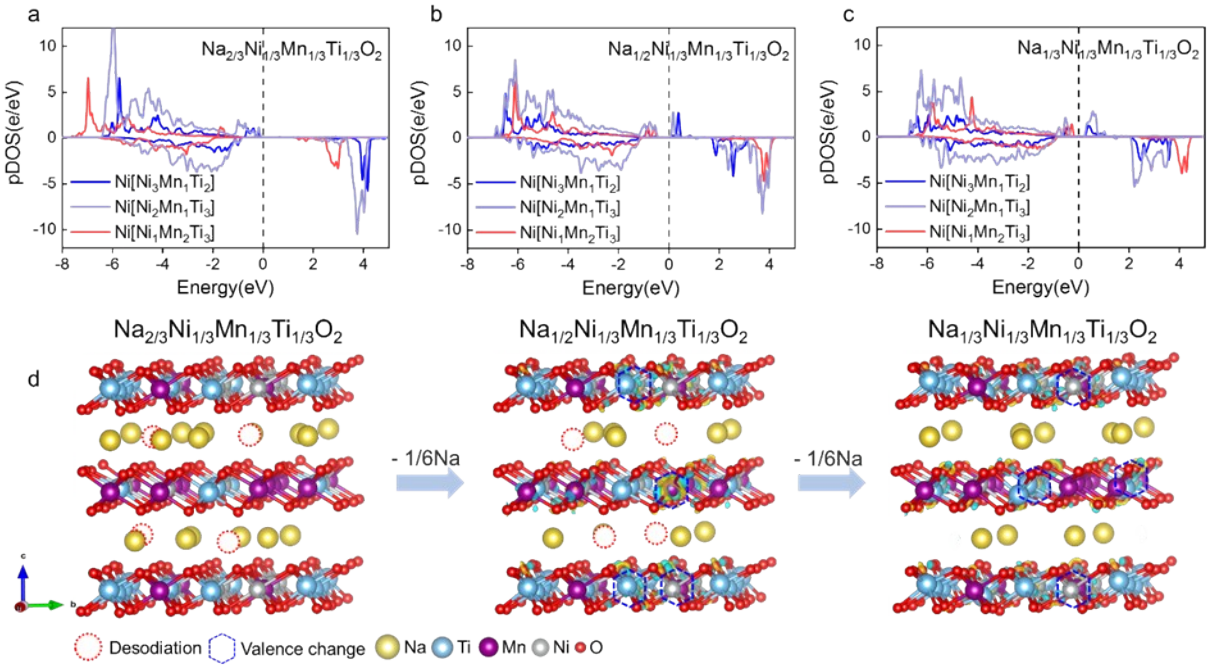

Figure S7. The behavior of $Na_{2/3}Ni_{1/3}Mn_{1/3}Ti_{1/3}O_2$ in the desodiation process. (a-c) The partial density of states of $Ni[Ni_3Mn_1Ti_2]$, $Ni[Ni_2Mn_1Ti_3]$ and $Ni[Ni_1Mn_2Ti_3]$ in $Na_{2/3}Ni_{1/3}Mn_{1/3}Ti_{1/3}O_2$ (x=0.67, 0.5, 0.33), respectively; (d) Structure evolution and charge-density difference of $Na_{2/3}Ni_{1/3}Mn_{1/3}Ti_{1/3}O_2$ (x=0.67, 0.5, 0.33) (yellow and blue represent positive and negative 0.0095 e/Å^3 isosurfaces, respectively) in the direction of a-axis.

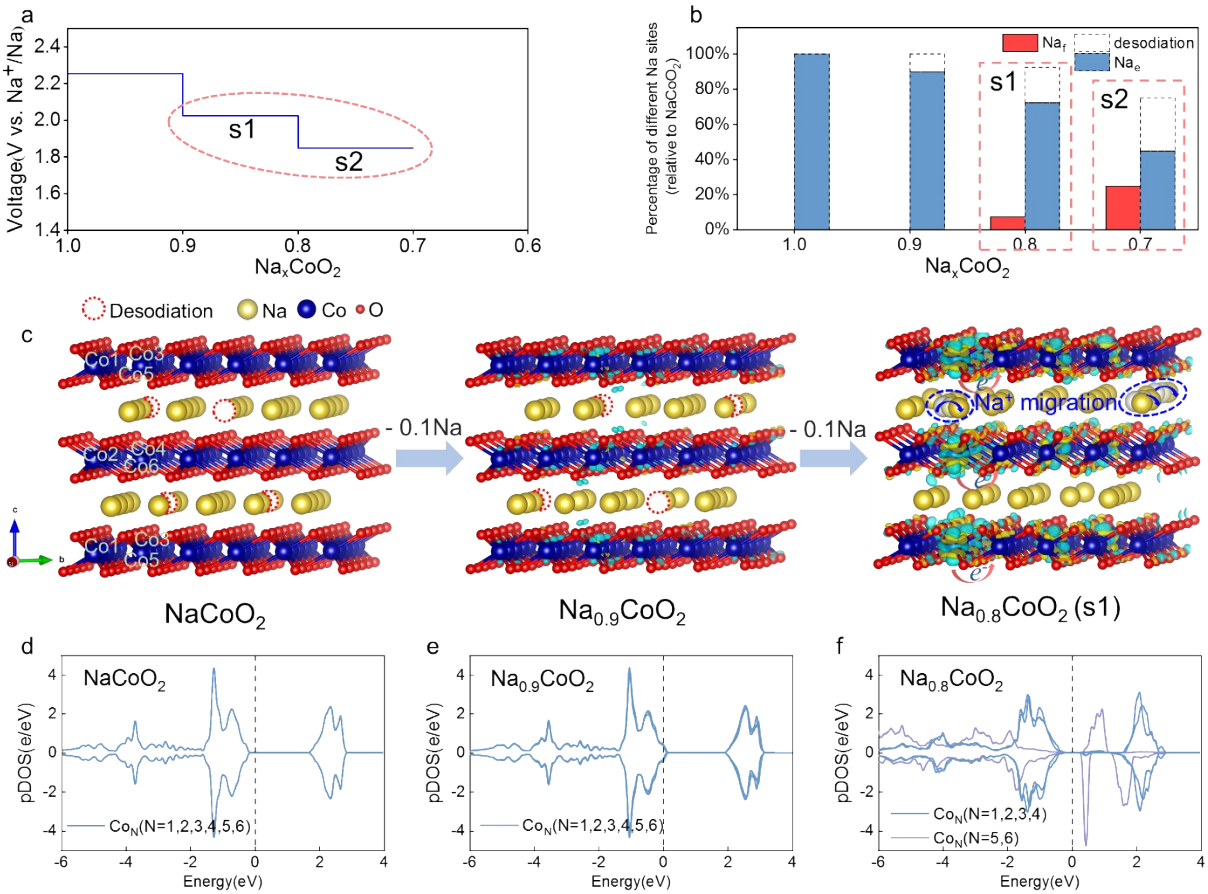

Figure S8. Behavior of P2-$NaCoO_2$ during the desodiation process. (a) Calculated voltage and charge transfer voltage of P2-$NaCoO_2$; (b) Changes in the two Na sites within the structure of Na_xCoO_2 (x = 1.0, 0.9, 0.8, 0.7) during the desodiation process. (c) Structure evolution and charge-density difference (yellow and blue represent positive and negative 0.006 e/Å^3 isosurfaces. respectively), typical Co1, Co2, Co3, Co4, Co5, Co6 are chosen as representatives to study the electronic structure changes. The directions of (c) are the a-axis direction. The blue arrows indicate the migration of sodium ions in (c) and the red arrows indicate the charge transfer of Co in (c); (d-f) The variation of the partial density of states of Co1, Co2, Co3, Co4, Co5, Co6 in different desodiation structures ($NaCoO_2$, $Na_{0.9}CoO_2$, $Na_{0.8}CoO_2$).